Eur Biophys J (1990) 19:47–54

European Biophysics Journal

Kinetic properties of single-ion channels activated by light in *Limulus* ventral nerve photoreceptors

K. Nagy

Institut für Biologie II der Rheinisch-Westfälischen Technischen Hochschule Aachen, Kopernikusstrasse 16, W-5100 Aachen, Federal Republic of Germany

Received May 21, 1990/Accepted in revised form August 31, 1990

Abstract. Previous results on *Limulus* ventral photoreceptors have suggested that besides inositol trisphosphate, another unknown transmitter may also work in the transduction cascade. This assumption has been supported by the finding of two light-activated channel types. The present report furnishes further evidence of the dual transmitter mechanism in phototransduction by analyzing the kinetic properties and voltage dependency of these cation channels with conductances of $\approx$12 pS and $\approx$30 pS. Single-channel currents were recorded in *Limulus* ventral nerve photoreceptors in cell-attached configuration at 14 °C. At $V_m \approx +80$ mV, the open-time histograms of both channels were fit best by the sum of two exponentials; time constants (and weights) were: 0.81 ms (0.62) and 6.20 ms (0.38) for the 12 pS channels and 2.38 ms (0.43) and 19.4 ms (0.57) for the 30 pS channels. At this potential the mean open times were 2.7 ms for the 12 pS and 13.3 ms for the 30 pS channels, about two-times larger than at hyperpolarizing potentials. The deactivation kinetics were also different for the two channels. The time constants of the decay of the channel activity, after switching off the light, were 2.5 s for the 12 pS and 12.9 s for the 30 pS channels. The 12 pS channel exhibits bursting and subconductance states at positive potentials. The subconductances are about 20%, 46% and 72% of the fully open state. Results show that the two types of light-activated channels have different kinetic parameters, voltage dependence and gating mechanisms. The two channels are suggested to be gated by different transmitters or processes. It is proposed that for the 30 pS channel the transmitter could be calcium ion or a calcium-dependent transmitter.

Key words: *Limulus* photoreceptor – Light-activated single channels – Single-channel kinetics

Introduction

Upon absorbing a photon, the rhodopsin molecule changes its conformation to an active meta state, which triggers an enzyme cascade, resulting in an increase in the concentration of a putative intracellular transmitter in *Limulus* ventral nerve photoreceptors (Cone 1973; Fein and Payne 1989; Becker et al. 1988; Stieve 1989). Transmitter molecules bind to channel proteins, causing their opening and leading to the depolarization of the photoreceptor cell. Receptor currents in *Limulus* photoreceptors are composed of several light- and voltage-dependent components (Fain and Lisman 1981). Lisman and Brown (1971 a) suggested that light activates two distinct ion currents, which are different in their kinetics and voltage dependence. Two components of the receptor potential and current could be distinguished in the course of dark adaptation (Maaz et al. 1981; Claßen-Linke and Stieve 1986), which were suggested to originate from two different light-activated channels. Pressure injection of calcium ions into the photoreceptor elicited rectified currents with reversal potential and ion selectivity similar to light-activated current (Payne et al. 1986 a). Therefore, it was suggested that the light- and calcium-activated currents arise from the same channel type. Injection of inositol 1,4,5-trisphosphate (IP_3) elicited a transient current similar to the light- and/or calcium-induced current (Payne et al. 1986 b). Therefore, IP_3, which releases calcium ions from intracellular stores (Fein et al. 1984; Brown et al. 1984), was suggested as an intracellular messenger. Payne et al. (1986 b) observed that injection of EGTA blocked the IP_3-induced, but not the light-induced current. Hence, they concluded that either the light has access to another pathway than IP_3 or light caused another transmitter to be released as well. It remains unclear, however, whether calcium directly activates channels or if it initiates the release of a terminal transmitter.

Getting over the difficulty of the patch-clamp technique with *Limulus* ventral nerve photoreceptor, Bacigalupo and Lisman (1983, 1984) and Bacigalupo et al. (1986) first measured single light-activated channels in this preparation. They reported a single-channel conductance of $\approx$40 pS, a channel open time of about 4 ms at negative potentials and a reversal potential of 10 mV. The reversal potential was similar to the value measured for

the macroscopic receptor current (Millecchia and Mauro 1969; Brown and Mote 1974), but the single channel conductance was larger and the channel open-time shorter than the values of 18 pS and 18 ms obtained from noise analyses (Wong 1978). The latency to the first openings measured from the onset of the light was very long and variable, up to several seconds, in contrast to the latencies of the single-photon responses, which are in the range of about 30 to 300 ms (Stieve 1986). The above discrepancies suggest that the 40 pS channel is probably not the only one that functions in the photoreceptors.

We reported recently (Nagy and Stieve 1990) that in *Limulus* ventral nerve photoreceptors, three different sizes of light-activated single-channel currents could be recorded. The single-channel conductances were found to be 6 pS, 10 pS and 29 pS at negative potentials. The most active channel had 10 pS conductance and the 6 pS channel was only rarely observed. Due to the different activation kinetics and channel open time, the 10 and 29 pS conductances were attributed to two different light-activated channel types, indicating two different intracellular mechanisms or transmitters.

The present paper describes the potential dependence of the 10 pS and the 29 pS channels and the kinetics of the channel activation and deactivation. These results give further evidence of distinct triggering mechanisms of the two channels and suggest that light activates two different transmitters or processes in this preparation. On the basis of the present results, previous unexplained electrophysiological effects can be interpreted.

Some parts of the results have been presented in a preliminary form (Nagy 1990).

Materials and methods

The methods have been partly described earlier (Nagy and Stieve 1990). Only new or essential detailes will be summarized here. The intracellular potential (V_i) of the dark-adapted cell was measured in several cells and found between -48 and -35 mV. During the 1-s illumination used in most of the experiments, V_i rapidly increased to about $+15$ mV (the time to peak is between 50 and 80 ms), but later ($t > 400$ ms) decreased to a steady-state value between -25 and -10 mV. If not otherwise stated, $V_i = -10$ mV was assumed for the estimation of the actual membrane potential V_m.

Single-channel currents were recorded in cell-attached configuration (Hamill et al. 1981) on the *R*-lobe of ventral nerve photoreceptors. Measurements were carried out either by holding the patch at a selected potential continuously, or by using voltage steps for 1 to 3 s from a holding potential. The step potential was switched on 300 to 500 ms before the light to avoid the drift of the baseline current elicited by the capacitive artifact during the light response. The constant holding potential was between 0 and -30 mV, relative to the cell's intracellular potential, V_i. Measurements were carried out at 14 °C; the maximum light intensity I_0 was 8 mW/cm^2 (white light).

Currents were filtered at 2 kHz (-3 dB, four-pole Bessel filter) and stored continuously in pulse-code modulated form (sampling frequency 44.1 kHz) on video tapes. Simultaneously, an IBM-compatible PC (AT-386, DATAC, FRG) was used for on-line measurements. The computer controlled the stimulus light, set the patch potential and sampled the current for 2.1 s at 10 kHz (by an AD converter, DAS-16 Metrabyte/Keithley Instruments, FRG) every 90 s.

For off-line analysis, either the records digitized at 10 kHz and stored on floppy discs were used, or segments of records stored on video tapes. To calculate the unitary conductance, single-channel current sizes were estimated from the usual amplitude histograms constructed from all points of a record range where the membrane potential had reached a steady-state value ($t > 500$ ms after switching on the light).

For studying the subconductance levels of the channels, conditional amplitude histograms were constructed by applying the variance-mean analysis (Patlak 1988). Records used for this calculations were digitized at 10 kHz. By this method the mean current and the variance were calculated for a segment of a record, called window, consisting of n sample points ($10 \leq n \leq 20$). The window was slid, point by point, over an interval of a current record, resulting in pairs of variance and mean current points. From these points a variance-mean plot was constructed (see Fig. 4 A). If the window contained transition points, short openings or closings (spikes), then the variance was large and the mean current somewhere between the closed and open value. Amplitude histograms were constructed from those points, which had smaller variance than the baseline, omitting transition points and spikes. In this conditional amplitude histogram, points from only those current segments were included that were longer than the window. For the present calculations windows containing 20 points (corresponding to 2.0 ms) were used. Programs used for the measurements and calculations were written by the author.

Open-time histograms were fitted by a single exponential or by the sum of two exponential functions using a least-squares fit algorithm. The mean open time (arithmetical mean value) for a histogram equals the time constant of a single exponential fit or is the weighted mean of the time constants for histograms best-fit by the sum of two exponential functions.

Results

Characterization of channels at negative and positive potentials

Figure 1 demonstrates the typical behavior of the light-activated channels at hyperpolarizing potentials. Channels opened with some delay after the onset of light and remained active for some time after switching off the light (discussed later). In Fig. 1 two different current sizes can be observed, indicating two populations of light-activated channels. Between $V_m \approx -40$ and $V_m \approx -100$ mV, the unitary conductances calculated from three patches were 11.7 pS (± 3.4) for the channel having the smaller current

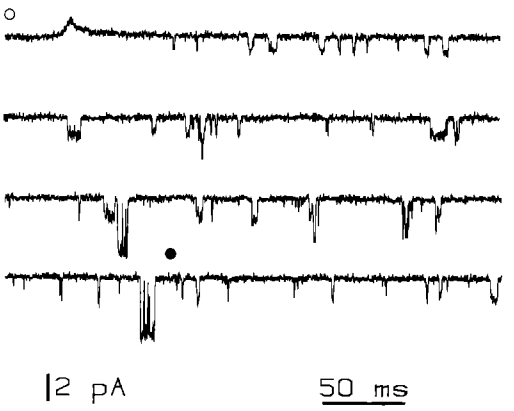

Fig. 1. Consecutive segments of a single channel current record measured in *Limulus* ventral photoreceptor in cell-attached configuration at $V_m \approx -90$ mV. (The exact membrane potential is $V_m = V_i - 80$ mV, where $V_i \approx -10$ mV, the cell's intracellular potential; see Materials and methods). The record demonstrates two different light activated channel types (called 12 pS and 30 pS channels). The inward currents are shown in negative direction. The patch was hyperpolarized for 3 s starting 500 ms before the first point of the record. The cell was illuminated for 1 s, from the *open circle* to the *closed one*. The light intensity was I_0, filter frequency 2 kHz and the sample frequency 10 kHz

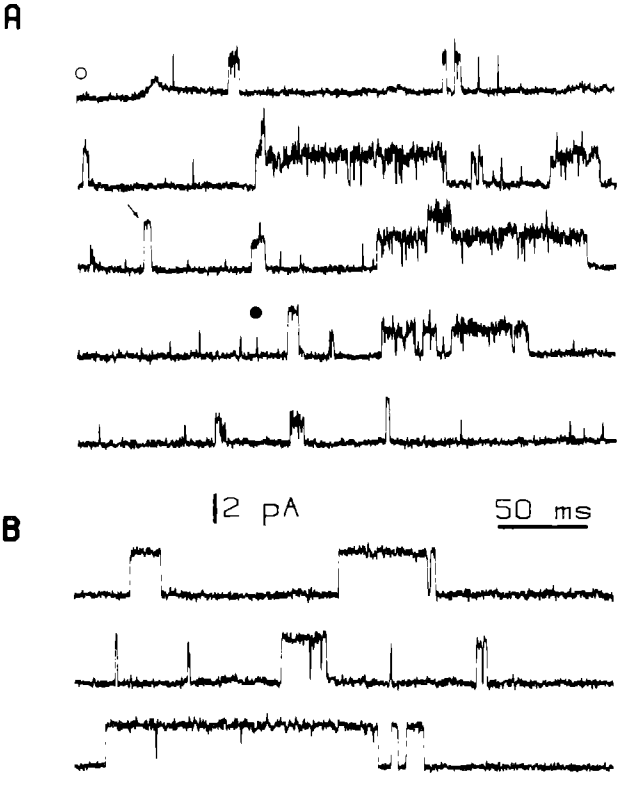

Fig. 2 A, B. Single-channel currents at positive potentials. **A** This record demonstrates outward currents (positive deflections) flowing through single and superimposed openings, as well as bursts of the 12 pS channel and single openings of the 30 pS channel. The first opening of the 30 pS channel is marked by an *arrow*. The cell (the same as in Fig. 1) was illuminated for 1 s from the *open circle* to the *closed one* with I_0 intensity. The membrane potential was $V_m \approx +90$ mV for 3 s set 500 ms before the first point. **B** Currents through the 30 pS channel measured with a light intensity of $I_0/50$ at the same pipette potential and in the same patch as in **A**. The cell was illuminated continously during the record. The light was switched on for 6 s, 3 s before the first point

size and 29.8 (± 4.1) pS for the channel having the larger current. A third channel with a conductance of ≈ 6 pS (Nagy and Stieve 1990) is not shown and will not be analyzed due to its rare appearance. The reversal potential was about 24 mV (absolute potential) for both channels. These parameters are similar to those reported earlier for the two channel types (Nagy and Stieve 1990).

Light-activated channels behave differently at depolarizing potentials (Bacigalupo et al. 1986). However, to study this question one must be sure that at strong depolarization only the light-activated and not voltage-gated channels are observed. Therefore, each patch was tested by consecutive depolarizing pulses (repetition time 90 s), alternating the addition or omission of stimulus light. Current records were analyzed for only the patches that did not show any activity in the dark in response to the depolarizing voltage steps.

Figure 2 A shows a current record from a patch clamped to $V_m \approx +90$ mV. Channels opened soon after the onset of the light and stayed active for some time in the dark after termination of the illumination, similar to the effect observed at negative potentials (Fig. 1). Two current amplitudes can be recognized in this record, indicating that the two channel types are active at positive potential as well. The 12-pS channel often exhibits bursting for long periods of time at depolarizing potentials. As the open-channel probability increased, the probability of finding overlapping openings increased as well (see trace 2 and 3 in Fig. 2 A). This channel was observed to burst for up to 500 ms. The increased noise during the openings of the 12 pS channel suggests that this channel flickers between the closed and open, or intermediate states (discussed later).

The 30 pS channel showed very different characteristics from that of the 12 pS channel. Occasionally, stimulations with moderate light intensities elicited exclusively the opening of the 30 pS channel, as illustrated in Fig. 2 B. This channel was sometimes open for up to 100 ms, showing neither short closed gaps nor flickering. The absence of flickering of the 30 pS channel is also indicated by the relatively small noise of the open channel current (compare the open channel current noise in Fig. 2 B to that of the 12 pS channel in Fig. 2 A).

Outward rectification was observed for both channel types at positive potentials. Between $V_m \approx +40$ mV and $V_m \approx +100$ mV, the conductances varied between 19 and 26 pS for the 12 pS and 36 to 48 pS for the 30 pS channels. (These estimations were made for three patches with three depolarizing potentials.)

The ratio of the number of openings for the 12 pS and 30 pS channels varied greatly for different patches and different potentials. The ratio of the number of 12 pS openings to number of 30 pS openings calculated for single-illumination periods ranged from 15 to 1.5 at negative potentials and from 35 to 0.05 at positive potentials (calculated in four patches).

Subconductance states of the 12 pS channel

Inspecting Fig. 2 A suggests that the bursting channel shows subconductance states. This question was studied

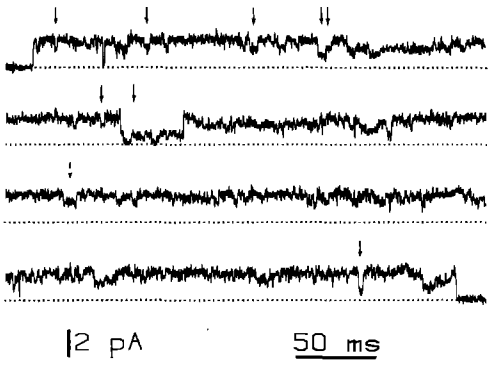

Fig. 3. A segment of a current record of a single-channel, demonstrating subconductance states of the 12 pS channel. The membrane potential was $V_m \approx +70$ mV. The light intensity was $I_0/50$ and the cell was illuminated for 6 s continuously during the record. Some of the substates are indicated by *arrows*

extensively on records, which showed clear, long subconductance states and only a few short gaps. Substates could be observed more frequently at moderate light intensities and depolarizations; however, this may be a coincidence. An example is shown in Fig. 3. The channel opens first to a fully open state, but later jumps to a substate, which has a conductance of about three-fourths of the fully open state. From this state, the channel can close and open again. Sometimes the current trace is unstable probably due to unresolved transitions between conductance states. Conductance levels of about half and one-fourth of the fully open state are also observed in Fig. 3.

Twelve current records were analyzed to show that the suspected sublevels are not due to a random distribution of current levels created by the limited time resolution of the measuring system. Channel openings showing subconductance states were omitted from the open-time histograms shown later.

The variance versus mean current plot obtained from two current records showing subconductance states is shown in Fig. 4 A (for calculation see Materials and methods). The roughly parabolic curves are due to the transitions between the current levels (see Patlak 1988). The incomplete curves with large variances indicate unresolved short closings or openings. The arrow on the ordinate marks the baseline variance. Current points having smaller variance than the baseline were selected for the conditional amplitude histogram shown in Fig. 4 B.

Conditional amplitude histograms showed five peaks (Fig. 4 B), corresponding to the currents that flowed at the closed state (i_0), the fully open (i_f) and the three substates (i_1, i_2, i_3). The amplitude histogram in Fig. 4 B could be best fit by the sum of five Gaussian functions (continuous line). The single-channel current levels (and the relative amplitudes in percent compared to the fully open state) are listed in the caption of Fig. 4. Similar relative current values were obtained for the other examples, but the relative appearance of the current levels were variable. The conductance level of $\approx 20\%$ (i_1) was expressed with the lowest frequency in each cases. The 100% and the $\approx 72\%$ conductances appeared with similar probability. This explains the large amount of noise in the open-channel current observed in Fig. 2 A, since the channel appears to flicker between the O_f and O_3 states, which correspond to the current sizes i_f and i_3.

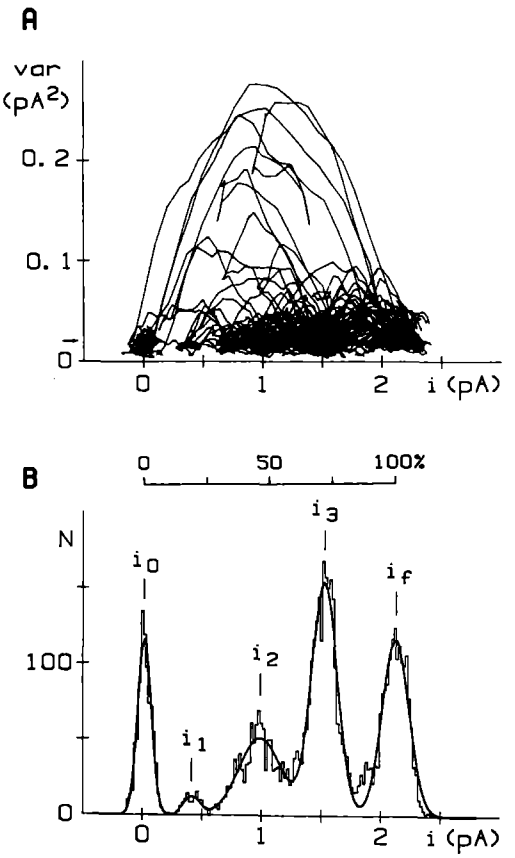

Fig. 4 A, B. Variance-mean analysis of the open channel currents (see Materials and methods) showing subconductance states. **A** Variance versus mean current plot obtained with a window width of 20 points. The *arrow* on the *ordinate* indicates the level of the baseline variance used as threshold (maximum value) for the construction of the conditional amplitude histogram shown in **B**. **B** Conditional amplitude histogram. The histogram was best fit by the sum of five Gaussian functions (*continuous line*). i_0 indicates the baseline current corresponding to the closed state. σ_0 was 0.06 pA. Open-channel currents (and relative sizes) are: at the fully open state, $i_f =$ 2.11 pA (100%) and at the substates $i_1 = 0.42$ pA (19.9%), $i_2 =$ 0.97 pA (46.0%), $i_3 = 1.51$ pA (71.6%). The standard deviations (σ) and the relative weights (w) of the components are: $\sigma_f = 0.11$ pA, $w_f = 0.34$, $\sigma_1 = 0.07$ pA, $w_1 = 0.02$, $\sigma_2 = 0.17$ pA, $w_2 = 0.23$, $\sigma_3 =$ 0.11 pA, $w_3 = 0.41$. $V_m \approx +70$ mV, $I = I_0/50$

Multiple current levels might also be due to superimposed openings of channels, but some aspects should be mentioned: (*a*) in all cases the largest current amplitude was first observed that would correspond to simultaneous opening of four channels; (*b*) several transitions from the $4x$, $3x$ and $2x$ levels to zero were observed; (*c*) single openings with $1x$, $2x$, or $3x$ levels were never observed. Therefore, it seems very probable that the multiple current levels are due to the substates of a single channel and not to simultaneous opening of independent channels. Synchronized gating of four channels, however, cannot be excluded.

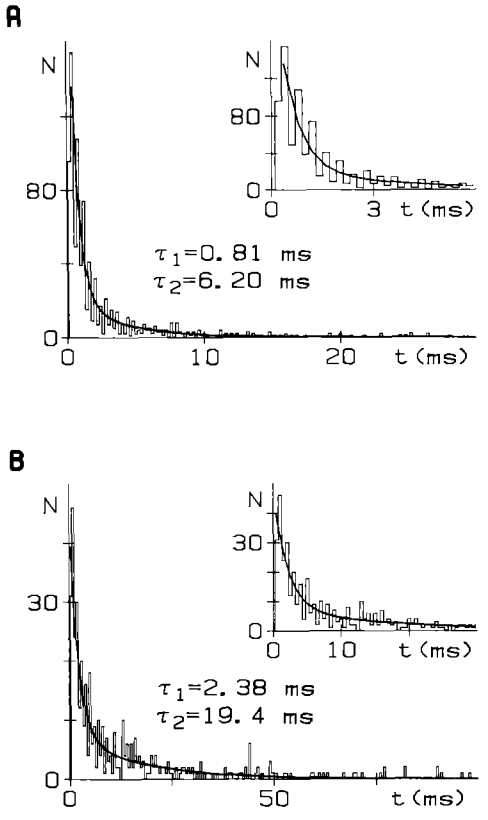

Fig. 5. **A** Open-time histograms of the 12 pS channel constructed from openings observed in a single patch at $V_m \approx +80$ mV. The fit resulted in time constants of τ_1 and τ_2, as indicated, and relative weights of 0.62 and 0.38. The mean open time was 2.73 ms; the number of events was 868. The *inset* shows the first part of the histogram and the fit on an expanded time scale. **B** Open-time histogram and its biexponential fit of the 30 pS channel calculated from the same patch at the same potential as plot A. The relative weights of the components are 0.43 and 0.57. The sum of events was 418; the mean open time was 13.3 ms. The bin width was 0.2 ms for both plots

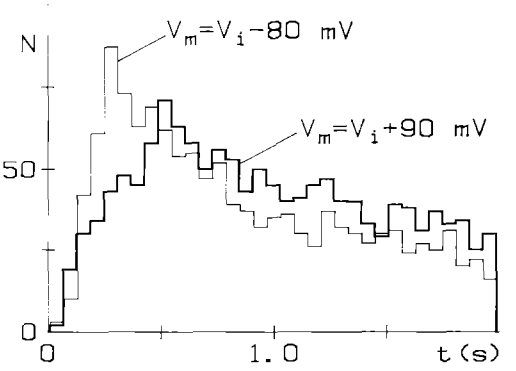

Fig. 6. Latency histograms of the 12 pS channel from a single patch at negative (*thin line*) and positive (*thick line*) membrane potential V_m. V_i was -15 mV. The bin width is 60 ms for both curves. The cell was illuminated for 1 s from time zero with light intensity of I_0

Channel open times

The open-time histogram of the 12 pS channel could be best fit by the sum of two exponential functions at negative potentials (Nagy and Stieve 1990), resulting in time constants of 0.58 ms and 4.32 ms at $V_m \approx -80$ mV. The mean open time was 1.65 ms (± 0.19 ms SEM) calculated from six patches. Bacigalupo et al. (1986) reported that the mean open time of the light-activated channels increased about four-fold at positive potentials. This property was studied for the two channel types analyzed here. The results indicate roughly a two-fold increase in the mean open time of the 12 pS channel from 1.65 ms at -80 mV to 2.73 ms at $V_m \approx +80$ mV.

In Fig. 5 A the open-time histogram of the 12 pS channels is shown for depolarization. The histogram was fit by the sum of two exponentials. The time constants of the fit was somewhat larger than those obtained at negative potentials (0.58 ms and 4.32 ms, respectively, from Nagy and Stieve 1990), and the relative weight of the slow component was increased by 58% from the value of 0.22, to 0.38.

Like the 12 pS channels, the open-time histograms of the 30 pS channels could also be best fit by the sum of two exponential functions at positive potentials (Fig. 5 B). A single exponential was sufficient for a good fit due to the low weight of the slow component at negative potentials, as previously reported (Nagy and Stieve 1990). At $V_m \approx -80$ mV the mean open times in the six patches used for these calculations were 5.19 ms (± 0.9 ms SEM) and at $+80$ mV 14.7 ms (± 1.2 ms SEM), indicating a 2.8-fold increase for the 160 mV potential change.

Latency of the 12 pS channel

It has been shown that the 12 pS channel opens with a short delay, about 50 ms, after the onset of the light at hyperpolarizing potentials (Nagy and Stieve 1990). The frequency of channel openings reached a maximum at about 300 ms, but later decreased. The time course of the channel activity observed at hyperpolarization and depolarization is compared in Fig. 6. The thick line indicates that the activity of the 12 pS channels increases slower at positive than at negative potential. This characteristic resembles the potential dependence of the time course of the macroscopic receptor currents, which reach a maximum later at positive potentials (see Fig. 8 in the paper of Bacigalupo et a. 1986). The channel activity decays after switching off the light (at 1.0 s) both at negative and positive potentials. The 30 pS channels opened with longer latencies than the 12 pS channels at both hyper- and depolarizations (see Figs. 1, 2 A), as reported earlier (Nagy and Stieve 1990).

Decay of the channel activity after the end of illumination

The 12 pS and 30 pS channels have different activation kinetics (Nagy and Stieve 1990). This suggests that they are gated by different transmitters or processes. If two processes have different activation kinetics, it is plausible to suppose that their relaxation kinetics are different as well. These kinetics can be studied by counting channel openings after switching off the stimulus light. It is as-

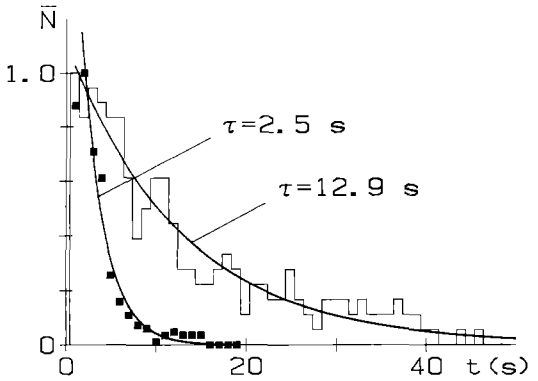

Fig. 7. Comparison of the decay of the activity of the 12 pS (*filled squares*) and the 30 pS channels (*step graph*) after switching off the light in a single patch. The histograms were normalized to the maximum for better comparison. The maximum for the *filled squares* was 82 events/s and for the *step graph* 18 events/s. The bin width was 1 s. Both histograms were fitted starting with the second bin because: (*a*) the number of events in the first second was sometimes uncertain due to the capacitive artifact elicited by the step potential that was switched off at this time and (*b*) in the first second some channels open due to the transmitters released in the last millisecond of illumination, i.e., at this time the transmitter concentration decay is slower (see Fig. 6A, B). The step potential was −20 mV; the steady holding potential was −10 mV. The cell was illuminated for 1 s with an intensity of I_0

sumed for this calculation that channels open fast relative to the kinetics of the transmitter concentration change. Figures 1, 2A and 6 show that the activity of channels did not stop instantaneously after switching off the light. The decay of the channel activity was studied at membrane potentials near the cells' dark potential, because these potentials (maximum ±20 mV voltage steps from the constant holding potential) did not change the behavior of the channels. An example is shown in Fig. 7. Here the normalized frequencies of channel openings for the 12 pS (filled squares) and the 30 pS channels (step graph) are compared. Both histograms could be best fit by a single exponential function, resulting in time constants of 2.5 s for the 12 pS and 12.9 s for the 30 pS channel. The mean values of the time constants for the four patches were 1.9 s (±0.6 s SEM) for the 12 pS and 13.7 s (±1.6 s SEM) for the 30 pS channels. The time constants of the decay of the activity are clearly different for the two channel types. This observation also supports that the 12 pS and 30 pS channels are gated by two different intracellular mechanisms or transmitters as suggested earlier (Nagy and Stieve 1990).

Discussion

This paper describes the single-channel parameters of two light-activated channel types in *Limulus* ventral nerve photoreceptors at hyper- and depolarizing membrane potentials. The two channels are different not only in unitary conductances, open time and activation kinetics (Nagy and Stieve 1990), but also in the voltage dependence of the single-channel parameters and, most important, in the time constants of the decay of the activity after illumination.

The 12 pS channel exhibits bursting (Fig. 2A) and subconductance states (Fig. 3) at positive potentials. Substates could not be observed at negative potentials, maybe due to the smaller probability of finding the channel in the open state. It should be noted that a ≈6 pS conductance channel occasionally observed (Nagy and Stieve 1990) has the half of the conductance of the 12 pS channel. However, those openings did not show transitions to other conductances; therefore, they are assumed to represent another channel type. The functional significance of the substates is unclear, but it is important for further studies of the structure and conformational changes of this molecule and for developing models. It is worth noting that the voltage-gated sodium channels in mouse neuroblastoma cells (Nagy 1987, 1988; Meves and Nagy 1989) and in muscle cells of mouse (Patlak 1988) also showed subconductance states with similar unitary steps of about one-fourth of the fully open state. These findings may indicate some structural similarity of the light-activated 12 pS channel (which is moderately sodium selective) to the voltage-gated sodium channel.

At positive potentials the mean open times of both the 12 pS and the 30 pS channels were increased about twofold compared to the value at negative potentials. However, the macroscopic light-activated conductance and open-channel probability have been reported to increase more than tenfold for positive potentials (Bacigalupo et al. 1986). The difference may be explained by the bursting behavior of the 12 pS channels (Fig. 2A) and the increased mean open time of the 12 pS and 30 pS channels.

The finding that the open-time histograms could be best fit by the sum of two exponential functions suggests that the 12 pS channel has two open conformations with different time constants and similar conductances, or that two populations of channels having similar conductances function in the cell. However, as this channel type exhibits a complex open conformation (see the subconductance states in Figs. 3, 4A and B), it seems to be more probable that one channel population exists with two kinetically distinct open states.

The most important finding of the present investigation is the different decay kinetics of the activity of the 12 pS and 30 pS channels after illumination (Fig. 7). This difference, together with the corresponding different time course of activation, supports the earlier suggestion (Nagy and Stieve 1990) that the two light-activated channel types are gated by different mechanisms or transmitters. The time constants reported here indicate the concentration decay of the two transmitters after the light is switched off, that is, after the production of the transmitters has stopped. The faster time constant (≈2 s) can be supposed to reflect the concentration decay (not necessarily the life time; see discussion later) of the intracellular transmitter gating the 12 pS channels. The slower time constant (≈13 s) corresponding to the activity decay of the 30 pS channel is in the range of the time constant of the dark adaptation (20 s, Fein and DeVoe 1973; 5–9 s, Claßen-Linke and Stieve 1986). As dark adaptation is regulated mainly by intracellular free calcium ions on this time scale (Lisman and Brown 1971b; Brown and Blinks 1974; Nagy and Stieve 1983; Levy and Fein 1985;

Claßen-Linke and Stieve 1986), it is suggestive that the 30 pS channels are gated by calcium ions or by a transmitter, the concentration of which is regulated by intracellular calcium ions. The time constant of the intracellular calcium concentration decay measured by arsenazo III in an unclamped cell is about 11.5 s (A. Deckert, personal communication), which is very close to the value calculated above, supporting the idea of the calcium-gated channels. A calcium-gated mechanism is in agreement with the observation of Payne et al. (1986), who reported that pressure injection of calcium elicits receptor currents that resemble the light-activated signals. An injection of EGTA blocked the signals elicited by calcium injection, but not the light-activated signals. It is suggestive that one of the channel types (probably the 12 pS channel) is excited by light in the presence of EGTA, indicating a transmitter that functions independently of intracellular calcium ions.

Assuming that the channel open time is shorter than the life time of the free transmitter (this assumption is probable because of the short channel open time), both the activity decay after illumination and the decay of the single photon responses (bumps) can be assumed to reflect the concentration decay of the transmitter (Bacigalupo and Lisman 1983; Dirnberger et al. 1985). The time constants of the activity decay of both channel types are much larger (factor >200) than the time constant of the decay of a single-photon response. It can be excluded that the difference is only due to the different experimental conditions, namely, the time constants become shorter with increasing illumination and intracellular calcium concentration. For light-adapted cells, the time constant of the bump decay was 12 ms and for dark-adapted cells it was 20 ms (Dirnberger et al. 1985). Single-channel currents were recorded with strong illumination, which should make the time constants even faster. To explain the large difference of more than two orders of magnitudes in the time constants, two hypotheses are suggested.

First, it can be assumed that the decay of the channel activity (presented here), but not the decay of the bump, reflects the lifetime of the transmitter. Then it should be assumed that the decay phase of the bumps reflects a slow phase of activation. This model is analogous to that of Aldrich et al. (1983), which explained the decay (inactivating) phase of the voltage-gated sodium current by a slow activation. The long lifetime of the transmitter could not be observed in bump experiments, because the transmitter molecules released by a single-absorbed photon diffuse and, after a bump (when the local concentration is low), they cause unsynchronized openings of channels, resulting in an increased baseline noise.

Secondly, it could be assumed that the time constant of the bump decay reflects the lifetime of the transmitter. In this case, it should be supposed that a large amount of transmitter is buffered during bright illumination and the time constants calculated from the activity decays of single channels correspond to the kinetic of the re-release of the transmitters.

Of the two hypotheses, the first seems to be more probable, but the second cannot be excluded either.

Acknowledgements. I wish to thank H. Stieve for his support and encouragement of this work and for stimulating discussions and comments on the manuscript. I thank M. Rack and A. Deckert for helpful discussions and comments on the manuscript. This work was supported by the Deutsche Forschungsgemeinschaft, Na 188/1-1.

References

Aldrich RW, Corey DP, Stevens CF (1983) A reinterpretation of mammalian sodium channel gating based on single channel recording. Nature 306:436–441

Bacigalupo J, Lisman JE (1983) Single-channel currents activated by light in *Limulus* ventral photoreceptors. Nature 304:268–270

Bacigalupo J, Lisman JE (1984) Light-activated channels in *Limulus* ventral photoreceptors. Biophys J 45:3–5

Bacigalupo J, Chinn K, Lisman JE (1986) Ion channels activated by light in *Limulus* ventral photoreceptors. J Gen Physiol 87:73–89

Becker UW, Nuske JH, Stieve H (1988) Phototransduction in the microvillar visual cell of *Limulus*: electrophysiology and biochemistry. In: Osborne N, Chader J (eds) Progress in retinal research, vol 8. Pergamon Press, Oxford, pp 229–253

Brown JE, Blinks JR (1974) Changes in intracellular free calcium concentration during illumination of invertebrate photoreceptors: detection with aequorin. J Gen Physiol 64:643–665

Brown JE, Mote MI (1974) Ionic dependence of reversal voltage of the light response in *Limulus* ventral photoreceptors. J Gen Physiol 63:337–350

Brown JE, Rubin LJ, Ghalayini AJ, Tarvel AL, Irvine RF, Berridge MJ, Anderson RE (1984) Myo-inositol polyphosphate may be a messenger for visual excitation in *Limulus* photoreceptors. Nature 311:160–162

Claßen-Linke I, Stieve H (1986) The sensitivity of the ventral nerve photoreceptor of *Limulus* recovers after light adaptation in two phases of dark adaptation. Z Naturforsch 41c:657–667

Cone RA (1973) The internal transmitter model of visual excitation, some quantitative implications. In: Langer H (ed) Biochemistry and physiology of visual pigments. Springer, Berlin Heidelberg New York, pp 275–282

Dirnberger G, Keiper W, Schnakenberg J, Stieve H (1985) Comparison of time constants of single channel patches, quantum bumps, and noise analysis in *Limulus* ventral photoreceptors. J Membrane Biol 83:39–43

Fain GL, Lisman JE (1981) Membrane conductances of photoreceptors. Progr Biophys Mol Biol 37:91–147

Fein A, DeVoe RD (1973) Adaptation in the ventral eye of *Limulus* is functionally independent of the photochemical cycle, membrane potential and membrane resistance. J Gen Physiol 61:273–289

Fein A, Payne R (1989) Phototransduction in *Limulus* ventral photoreceptors: roles of calcium and inositol trisphosphate. In: Stavenga DG, Hardie RC (eds) Facets of vision. Springer, Berlin Heidelberg New York, pp 173–185

Fein A, Payne R, Corson DW, Berridge MJ, Irvine RF (1984) Photoreceptor excitation and adaptation by inositol 1,4,5-trisphosphate. Nature 311:157–160

Hamill OP, Marty A, Neher E, Sakmann B, Sigworth FJ (1981) Improved patch clamp techniques for high-resolution current recording from cells and cell-free membrane patches. Pflügers Arch Eur J Physiol 391:85–100

Levy S, Fein A (1985) Relationship between light sensivity and intracellular free Ca concentration in *Limulus* ventral photoreceptors. A quantitative study using Ca-selective microelectrodes. J Gen Physiol 85:805–841

Lisman JE, Brown JE (1971a) Two light-induced processes in the photoreceptor cells of *Limulus* ventral eye. J Gen Physiol 58:544–561

Lisman JE, Brown JE (1971b) The effects of intracellular Ca^{2+} on the light response and on light adaptation in *Limulus* ventral photoreceptors. In: Arden GB (ed) The visual system: neuro-

physiology, biophysics and their clinical applications. Plenum Press, New York, p 21

Maaz G, Nagy K, Stieve H, Klomfaß J (1981) The electrical light response of the *Limulus* ventral nerve photoreceptor, a superposition of distinct components – observable by variation of the state of light adaptation. J Comp Physiol A 141:303–310

Meves H, Nagy K (1989) Multiple conductance states of the sodium channel and of other ion channels. Biochim Biophys Acta 988:99–105

Millecchia R, Mauro A (1969) The ventral photoreceptor cells of *Limulus*. III. A voltage clamp study. J Gen Physiol 54:331–351

Nagy K (1987) Subconductance states of single sodium channels modified by chloramine-T and sea anemone toxin in neuroblastoma cells. Eur Biophys J 15:129–132

Nagy K (1988) Mechanism of inactivation of single sodium channels after modification by chloramine-T, sea anemone toxin and scorption toxin. J Membrane Biol 106:29–40

Nagy K (1990) Kinetics of two types of light activated single channels in *Limulus* ventral nerve photoreceptors. 10th International Biophysical Congress, Vancouver, (BC abstr), p 481

Nagy K, Stieve H (1983) Changes in intracellular calcium ion concentration, in the course of dark adaptation measured by arsenazo III in the *Limulus* photoreceptor. Biophys Struct Mech 9:207–223

Nagy K, Stieve H (1990) Light-activated single channel currents in *Limulus* ventral nerve photoreceptors. Eur Biophys J 18:221–224

Payne R, Corson DW, Fein A (1986a) Pressure injection of calcium both excites and adapts *Limulus* ventral photoreceptors. J Gen Physiol 88:107–126

Payne R, Corson DW, Fein A, Berridge MJ (1986b) Excitation and adaptation of *Limulus* ventral photoreceptors by inositol 1,4,5 trisphosphate result from a rise in intracellular calcium. J Gen Physiol 88:127–142

Patlak JB (1988) Sodium channel subconductance levels measured with a new variance-mean analysis. J Gen Physiol 92:413–430

Stieve H (1986) Bumps, the elementary excitatory responses of invertebrates. In: Stieve H (ed) The molecular mechanism of photoreception. Springer, Berlin Heidelberg New York, pp 199–230

Stieve H (1989) Microvillar photoreceptor cells of invertebrates. In: Torre V, Cervetto L (eds) Sensory transduction. Plenum Press, New York, pp 109–124

Wong F (1978) Nature of light-induced conductance changes in ventral photoreceptors of *Limulus*. Nature 276:76–79